

Discovery of CRN04894: A Novel Potent Selective MC2R Antagonist

Sun Hee Kim,* Sangdon Han, Jian Zhao, Shimiao Wang, Ana Karin Kusnetzow, Greg Reinhart, Melissa A. Fowler, Stacy Markison, Michael Johns, Rosa Luo, R. Scott Struthers, Yunfei Zhu, and Stephen F. Betz



Cite This: <https://doi.org/10.1021/acsmmedchemlett.3c00514>



Read Online

ACCESS |



Metrics & More



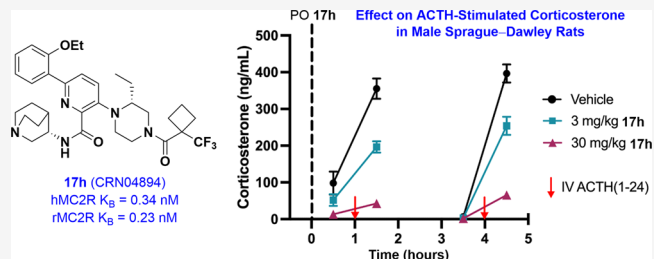
Article Recommendations



Supporting Information

ABSTRACT: A novel class of nonpeptide melanocortin type 2 receptor (MC2R) antagonists was discovered through modification of known nonpeptide MC4R ligands. Structure–activity relationship (SAR) studies led to the discovery of **17h** (CRN04894), a highly potent and subtype-selective first-in-class MC2R antagonist, which demonstrated remarkable efficacy in a rat model of adrenocorticotrophic hormone (ACTH)-stimulated corticosterone secretion. Oral administration of **17h** suppressed ACTH-stimulated corticosterone secretion in a dose-dependent manner at doses ≥ 3 mg/kg. With its satisfactory pharmaceutical properties, **17h** was advanced to Phase 1 human clinical trials in healthy volunteers with the goal of moving into patient trials to evaluate CRN04894 for the treatment of ACTH-dependent diseases, including congenital adrenal hyperplasia (CAH) and Cushing's disease (CD).

KEYWORDS: MC2R antagonist, ACTH, Corticosterone, Cushing's disease, CAH



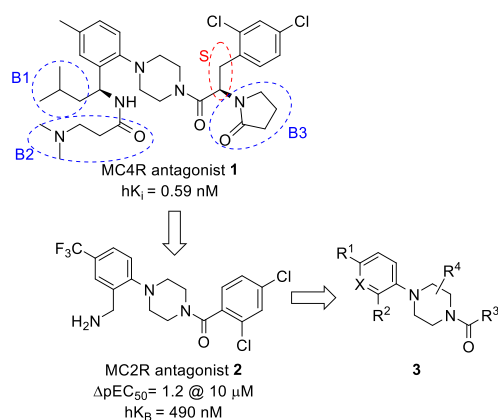


Figure 1. Structural modification to convert functional selectivity from an MC4R antagonist to an MC2R antagonist.

starting point. Compound **1** has potent MC4R binding affinity, which may be driven by specific branches (B1, B2, and B3), a spacer (S), or a combination of both.¹¹ The first step in attempting to convert the functional antagonist activity from MC4R to MC2R was to simplify structure **1** by deleting B1–3. This attempt did not result in MC2R antagonism. The propionyl spacer, S, was also modified. The two-carbon ethylene linker was removed, and an aryl group was directly attached to the amide carbonyl group to yield derivative **2**. This structural change resulted in successful conversion of functional MC4R antagonism to MC2R antagonism.¹² Compound **2** exhibited MC2R antagonism ($K_B = 490$ nM) and was further optimized as generalized structure **3** depicting various areas of a potential structure–activity relationship (SAR).

Structure **3** was the subject of multiple SAR investigations including R¹, R², R³, R⁴, and X individually and in combination. As a result, we discovered a novel series of potent and selective MC2R antagonists that culminated in clinical candidate **17h** (CRN04894). Herein, we disclose the detailed discovery process from the starting point (**2**) to the clinical candidate

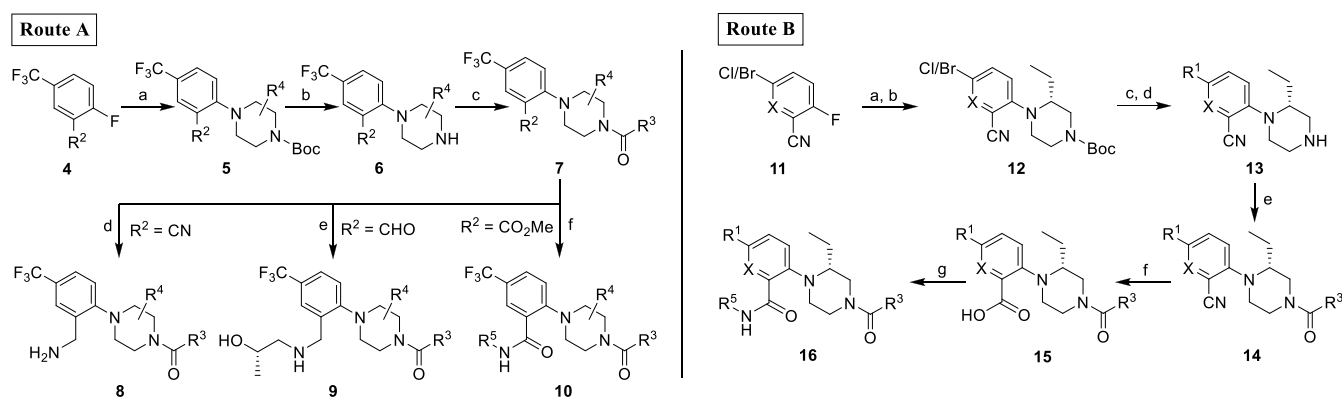
(**17h**), including in vitro pharmacological and in vivo pharmacokinetic and pharmacodynamic characterization to support it as a potential treatment of CAH and CD in humans.

To enable our SAR strategy, a series of analogues were prepared starting from commercially available compounds **4** or **11**, as illustrated in Scheme 1. Route A was used to provide analogues of structures **8–10** in Table 1. Beginning with readily available compound **4**, various R⁴-substituted piperazines displaced the reactive fluorine group via an S_NAr reaction, providing intermediate **5** in good yields. Removing the Boc protecting group was accomplished under acidic conditions to free the N-4 piperazine nitrogen. The resultant unprotected piperazine was converted to an amide by either a HATU-mediated coupling reaction with an acid or an electrophilic substitution with an acid chloride. The amide **7** was then subjected to three different reactions to give **8**, **9**, or **10**, based on the functionality of R². Depending on R², the reactions were nitrile reduction, reductive amination of an aldehyde, or consecutive ester hydrolysis and amidation.

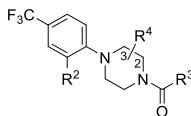
Route B was more extensively employed because it allowed for simultaneous SAR evaluation on groups R¹, R³, and R⁵. The synthetic route in Route B paralleled that from Route A but differed in two significant ways. The first was an additional Suzuki cross-coupling of **12** with the appropriate boronic acid or ester to introduce R¹ in lieu of the CF₃ group of **6**. This synthetic strategy employed a mixture of bromo- and chloro-substituted starting materials **11**. The second difference was the use of a nitrile hydrolysis instead of the ester hydrolysis to introduce the carboxylic acid precursor **15**. The hydrolysis of nitrile to carboxylic acid was performed with KOH under a binary solvent system of water and ethanol. As stated above, the more flexible Route B allowed the SAR at R¹, R³, and R⁵ and potentially R⁴.

Using synthetic Route A, we obtained the analogues in Table 1. Compounds were tested in a functional HTRF cAMP assay to measure any potency shift (ΔpEC₅₀) of ACTH in the presence and absence of a standard concentration of the compound. This ΔpEC₅₀ was often used as an initial estimate of compound potency. In addition, a competition binding

Scheme 1. Representative Synthesis^a



^aRoute A: Reagents and conditions: (a) *tert*-butyl R⁴-piperazine-1-carboxylate, DIEA, DMF or DMSO, 125–130 °C, 5–15 h; (b) HCl or TFA, DCM, rt, 1–2 h; (c) R³CO₂H, HATU, DIEA, DMF, rt, 20 min or R³COCl, TEA, DCM (or THF), rt, 30 min; (d) NaBH₄, NiCl₂, EtOH, rt, 2 h; (e) corresponding amine, NaBH₃CN, AcOH, MeOH, rt, 15 h; (f) LiOH·H₂O, H₂O/MeOH/THF (1:1:3), rt, 8 h, followed by amine, HATU, DIEA, DMF, rt, 30 min. Route B: Reagents and conditions: (a) *tert*-butyl (R)-3-ethylpiperazine-1-carboxylate, DIEA, DMSO, 140 °C, 2 d; (b) Boc₂O, DIEA, rt, 1 h; (c) R¹B(OR)₂, Pd(amphos)Cl₂, K₂CO₃, dioxane/H₂O (10:1), 100 °C, 1 h; (d) TFA, DCM, rt, 1 h; (e) R³CO₂H, HATU, DIEA, DMF, rt, 10–30 min; (f) KOH, H₂O/EtOH (1:1), 100 °C, 15 h; (g) corresponding amine, HATU, TEA (or DIEA), MeCN (or DMF), rt, 30 min.

Table 1. Optimization of Variants, R² and R⁴

cpd	R ²	R ⁴ -piperazine	R ³	human pK _B	human K _B , ^a nM (ΔpEC ₅₀) ^b	rat pK _B	rat K _B , ^a nM (ΔpEC ₅₀) ^b
8a				6.4 ± 0.1	390	–	–
8b				6.1 ± 0.1	830	–	–
8c				6.5 ± 0.1	300 (2.1)	–	–
8d				–	(0.6)	–	–
8e				7.7 ± 0.2	20	–	(1.0)
9a				7.6 ± 0.2	26	6.6 ± 0.3	252 (1.5)
10a				7.6 ± 0.2	23	7.1 ± 0.1	78

^aK_B values are the mean of two or more independent experiments. ^bAssay using CHO-K1 cells stably expressing the MC2R/MRAP complex: potency shift (ΔpEC₅₀) is the difference between the pEC₅₀ for ACTH stimulated cAMP synthesis in the presence and absence of 10 μM compound (human MC2R) and 3 μM compound (rat MC2R): ΔpEC₅₀ = (ACTH pEC₅₀ no compound) – (ACTH + 10 μM or 3 μM compound pEC₅₀).¹³

assay using [[¹²⁵I]-Tyr²³] ACTH (1–39) was used to measure K_i. Compounds with significant potency shifts (ΔpEC₅₀ > 2) or with potent binding affinities were further tested in a functional antagonist assay to determine the K_B of the compounds.

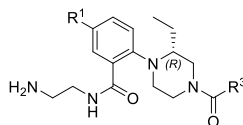
A CF₃ group at R¹ was held constant in Markush structure 3 while R², R³, and R⁴ were varied. Based on the preliminary study of R³ on structure 7, *ortho* and *para* disubstituted phenyl groups were preferred based on the increased potency observed with this pattern. *Ortho* and *para* disubstituted phenyl groups at R³ were held constant while groups R² and R⁴ were modified. The first focus was on the central piperazine spacer of structure 8 to explore the optimal substitution for R⁴. A methyl substitution survey of the two regioisomeric centers of piperazine in **8a–b** revealed a small binding preference toward the 3-position. Next, the stereogenic preference of the 3-methyl group was evaluated in **8c–d**, with the (3*R*)-designation to be the favored stereochemistry, affording an improvement in affinity from the starting point (**2**). Surprisingly, homologating the (3*R*)-ethyl group in **8e** from its (3*R*)-methyl analogue **8c** enhanced binding 15-fold.

The next SAR study was focused on R². The plan included extending the terminal benzylamine of R² on **8e**. For instance, the primary amine was converted to a secondary amine by substitution with a hydroxyethyl group in **9a**. This change did not add meaningful affinity in human MC2R but contributed

to a slight positive potency shift in rat MC2R. Rat ΔpEC₅₀ of **9a** is 1.5 while that of **8e** is 1.0. Nonetheless, potency differences between species remained (hK_B = 26 nM vs rK_B = 252 nM). The species selectivity was reduced to 3-fold when a benzylamine moiety of **8e–9a** was transformed to a benzamide in **10a**.

Further optimization efforts on R² of **10a** were continued and were unsuccessful in improving the potency beyond the double-digit nanomolar range. We then visited the R¹-CF₃ group on structure **10a** and replaced it with different aryl groups R¹, exploring the possibility that additional binding interactions could be obtained via substitution on the aromatic ring. The SAR activities are summarized in Table 2. With optimized R² and R⁴ substituents on **10a**, preferred substitution patterns on the aryl moiety R¹ were screened to afford variously substituted analogues **16a–e**. Electron withdrawing groups (EWGs) at the *ortho*-position in **16a–c** were characterized by weaker potency than the electron donating group (EDG) in **16e**, although the potency order was not well correlated with EW strength. Additional *meta*-fluoro substitution had a negligible effect in **16d** as compared to that in **16b**. A significant effect on potency was observed with the *o*-ethoxy group (**16e**), which provided the first analogue with single-digit nanomolar potency.

With the optimized *o*-ethoxyphenyl moiety, R³ was further explored (**16f–g**). In this SAR study, *o*-trifluoromethyl-*p*-

Table 2. Optimization of R¹ and R³

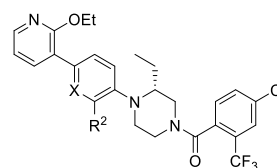
cpd	R ¹	R ³	human pK _i	human K _i ^a (nM)
16a			7.3 ± 0.1	47
16b			7.7 ± 0.1	21
16c			7.6 ± 0.0	25
16d			7.4 ± 0.0	36
16e			8.7 ± 0.0	2.0
16f^b			8.3 ± 0.0	4.8
16g			8.8 ± 0.1	1.6
16h			8.9 ± 0.0	1.1

^aK_i values are the mean of two or more independent experiments.

^bPK parameters with 10 mg/kg cassette PO dose in rat: C_{max} = 2.8 nM, AUC_(0-t) = 8.1 nM·h.

chlorophenyl **16g** had the same potency range as that of **16e**. Considering the minimal activity loss of an extra *meta*-F substitution in **16d**, the 3-pyridyl moiety was used as a bioisosteric replacement for the R¹ phenyl ring on **16g**. This resulted in **16h** with a 2-ethoxy-3-pyridyl moiety that was well tolerated like **16g**. Additionally, the 3-pyridyl moiety provided the added benefits of lowering lipophilicity and improving the overall physicochemical properties.

However, several of these analogues have poor oral exposure in rat pharmacokinetic (PK) studies. For example, compound **16f** was dosed by cassette PO and displayed a low AUC (see footnote *b* in Table 2). We believe that the low oral exposure is likely a result of low permeability of the molecule because of a relatively high proton donor count from its R² amide and terminal primary amine. As a strategy to improve oral bioavailability, we tried two SAR strategies in parallel to give analogues in Table 3. The first approach was to substitute proton donors of the primary amine with one or more methyl groups to afford either secondary or tertiary amine analogues (**16i–j**). **16i–j** maintained a similar potency to that of its primary amine analogue (**16h**). The second strategy was to mask the proton donor from the amide group by intramolecular hydrogen bonding. This was accomplished by replacing the neighboring X group from CH with either CF or nitrogen, which yielded **16k–l**. Analogues **16k–l** led to

Table 3. Optimization of R² and X and Identification of Advanced Lead, **16n**

cpd	X	R ²	human pK _i	human K _i ^a (nM)
16i	CH		9.0 ± 0.1	0.96
16j^b	CH		8.8 ± 0.2	1.5
16k^b	CF		9.0 ± 0.1	0.90
16l^b	N		9.4 ± 0.1	0.39
16m	N		9.3 ± 0.1	0.47
16n	N		9.5 ± 0.3	0.30
16o	N		9.5 ± 0.1	0.32

^aK_i values are the mean of two or more independent experiments.

^bLipE = 2.8 for **16j**, 3.1 for **16k**, and 4.4 for **16l**.

Table 4. Pharmacokinetic Properties of **16l–o** in Rat and Liver Microsomal (LM) Stability

cpd	form	pharmacokinetic PO parameters ^a			LM, t _{1/2} (min) ^c	
		t _{1/2} ^b (h)	AUC _{last} (nM·h)	F (%)	human (min)	rat (min)
16l	Parent	1.6	349	8	23	21
16m	Metabolite	2.7	334		>693	231
16n	Parent	2.2	1443	17	35	43
16o	Metabolite	4.0	279		231	347

^aDose 5 mg/kg (IV) and 10 mg/kg (PO) in 100% PG formulation.

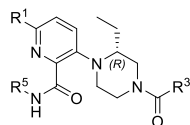
^bValues are total. ^cLiver microsomal stability, half-life (t_{1/2}).

moderate to high increases in potency. In addition to the primary strategy of reducing the number of proton donors, we implemented an additional strategy to improve the bioavailability of the series by reducing the number of rotatable bonds. Here, replacement of the acyclic amine (**16l**) with a pyrrolidine moiety (**16n**) of the basic amine side chain maintains good potency.

Compounds **16l** and **16n** were chosen for PK studies, and their PK parameters are shown in Table 4. Both **16l** and **16n** were not stable in liver microsomes, likely due to the tertiary amine on R². Further investigation demonstrated that monodesmethylation of the tertiary amine formed the corresponding secondary amine byproduct as the major active metabolites **16m** and **16o**, respectively.

Therefore, we collected both parent and metabolite information in the study to provide AUC values. The metabolically more stable **16n** showed more parent **16n** (AUC_{last} = 1443 nM·h) than metabolite **16o** (AUC_{last} = 279 nM·h) in the plasma as compared to the less stable **16l**. In addition, the strategy of reducing the number of rotatable bonds and restricting molecular flexibility by installing the

Table 5. Lead Optimization and Identification of Clinical Candidate, 17h



cpd	R ¹	R ⁵	R ³	human pK _i	human K _i ^a (nM)	human pK _B	human K _B ^a (nM)	LM t _{1/2} ^b (min)
17a				9.2 ± 0.1	0.63	8.9 ± 0.2	1.4	23 (h) 231 (r)
17b				8.4 ± 0.2	3.7	8.9 ± 0.1	1.4	77 (h) >693 (r)
17c				9.4 ± 0.1	0.40	9.5 ± 0.1	0.34	69 (h) 32 (r)
17d				8.5 ± 0.1	3.0	8.7 ± 0.2	2.1	–
17e				8.4 ± 0.1	4.4	–	–	–
17f				8.8 ± 0.0	1.6	8.7 ± 0.0	2.1	–
17g				8.9 ± 0.2	1.3	8.8 ± 0.2	1.6	116 (h) 231 (r)
17h				8.7 ± 0.1	2.1	9.5 ± 0.1	0.34	231 (h) 231 (r)

^aK_i and K_B values are the mean of two or more independent experiments. ^bLiver microsomal stability, half-life (t_{1/2}).

Table 6. In Vitro Selectivity of Compound 17h

species MC2R, pK _B (K _B) ^a			human MCR1–5, IC ₅₀ (μM)			
human	rat	dog	MC1R	MC3R	MC4R	MC5R
9.5 ± 0.1 (0.34 nM)	9.6 ± 0.1 (0.23 nM)	9.6 ± 0.1 (0.25 nM)	>10	>1.0	>10	>1.0

^aK_B values are the mean of two or more independent experiments.

Table 7. In Vitro ADME Properties of Compound 17h

LM, t _{1/2}	hERG	CYP450, IC ₅₀ (μM)				MDCK		PPB, %bnd ^c @ 1 μM		
dog	patch clamp	2C9 Inh.	2C19 Inh.	2D6 TDI	3A4 TDI	P _{app} ^a (10 ^{−6} cm/s)	MDR1 ER ^b	human	rat	dog
173 min	19 μM	>10	>10	>10	>10	1.9	95	98.6	97.4	86.8

^aPassive permeability. ^bMDR1 efflux ratio (B to A)/(A to B). ^cPlasma protein bound (bnd).

Table 8. Pharmacokinetic Properties of Compound 17h

species	IV		PO			
	CL (L/h/kg)	V _{ss} (L/kg)	t _{1/2} (h)	C _{max} (nM) ^c	AUC _{last} (nM·h) ^c	F (%)
rat ^a	1.47	3.19	2.73	1217	5201	47
dog ^b	0.85	10.50	9.55	650	4971	100

^aIV: 5 mg/kg, 10% (v/v) ethanol in water; PO: 10 mg/kg, 100% propylene glycol (PG). ^bIV: 2.5 mg/kg, 10% (v/v) ethanol in water; PO: 5 mg/kg, 100% PG. ^cValues are total.

cyclic pyrrolidine in **16n** resulted in both greater exposure and higher oral bioavailability, and **16n** was selected as a key compound for advanced profiling.

Subsequent studies revealed safety liabilities for **16n**. The safety findings with **16n** triggered a drive to potentially

mitigate toxicological liabilities by reducing the aromatic ring count as the next direction for lead optimization.

The final SAR campaign incorporated key elements identified from previous studies and focused on the replacement of aromatic rings with aliphatic structural bioisosteres. Modifying the aryl terminal pieces on either R¹ or R³ was possible. However, the R¹ aryl group was shown to be crucial for potency as previously described (Table 2), and therefore, the R³ aryl group became the target for an aliphatic surrogate.

The SAR work with R³ was focused on an achiral piece, and these efforts provided three representative compounds **17a–c** with decent potency. The small cyclobutyl group met the criteria of acceptable microsomal stability, but the potency needed to be enhanced. Having 1-(trifluoromethyl)cyclobutyl R³, we examined piperidyl and (S)-quinuclidine amines in

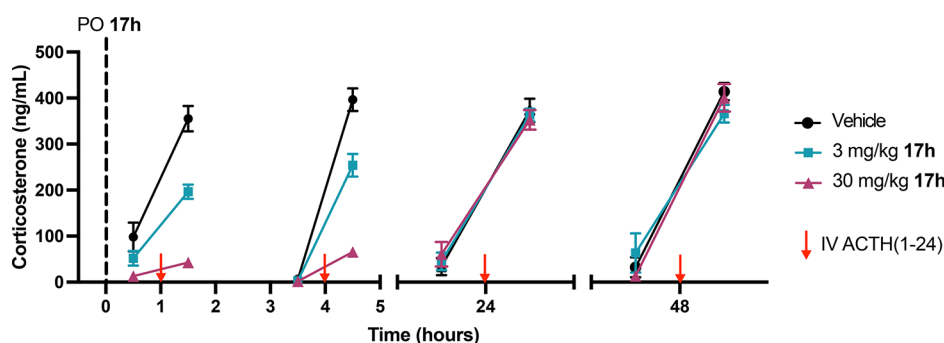


Figure 2. Effect of oral 17h on ACTH-stimulated corticosterone after a single administration in male Sprague–Dawley rats. Mean (SEM) plasma corticosterone levels measured at –30 and 30 min post-IV administration of 1 mg/kg ACTH(1–24) at 1, 4, 24, and 48 h (denoted by red arrows) post a single oral administration of vehicle or 3 or 30 mg/kg 17h in male Sprague–Dawley rats.

Table 9. Plasma Concentrations of 17h Following a Single Oral Administration

17h dose (mg/kg)	plasma 17h concentration (ng/mL) per time point ^a							
	1 h ACTH-stim test		4 h ACTH-stim test		24 h ACTH-stim test		48 h ACTH-stim test	
	0.5 h	1.5 h	0.5 h	1.5 h	0.5 h	1.5 h	0.5 h	1.5 h
3	110	93.9	127	87.5	0.927	0	0	0
30	1140	1530	1460	1260	20.0	14.1	0.880	0

^aData represented as mean values of 7–8 rats/group. Relative to ACTH administration.

17d–e, which remained similarly potent as the pyrrolidine amine in 17b. When these three amines were reexamined with the pyridyl moiety interchanged with *o*-ethoxyphenyl at the R¹ residue, all three compounds (17f–h) exhibited no to minimal enhancement in potencies in our binding assay. However, compound 17h exhibited desirable functional potency ($hK_B = 0.34$ nM) as well as microsomal stability. Compound 17h was further evaluated for in vitro and in vivo pharmacology, ADME properties, and pharmacokinetic properties.

Functional data demonstrated that 17h potently inhibited ACTH-driven cAMP production via human MC2R with an average equilibrium constant of binding in a functional assay (K_B) of 0.34 nM. Compound 17h also inhibited ACTH-stimulated cAMP accumulation via rat and dog MC2R activation with K_B s of 0.23 and 0.25 nM, respectively. Selectivity over other human melanocortin subtypes was evaluated using MC1R, MC3R, MC4R, and MC5R membrane binding assays. The half-maximal inhibitory concentration in the binding assays (IC_{50}) was determined to be greater than the highest concentrations tested (Table 6).

In addition to melanocortin receptor-directed pharmacology, 17h was also evaluated in an expanded selectivity panel of 87 assays that included a variety of GPCRs, enzymes, ion channels, and transporters known to be important counter screens for off-target activity in drug discovery. Compound 17h, tested at 10 μ M, showed little activity across the panel. Only the serotonin 5-hydroxytryptamine 1B receptor (5-HT_{1B}), calcium channel L-type, and sodium channel showed inhibition/activity of >70% at this concentration (Table S1). Subsequent dose–responses of 17h against the 5-HT_{1B} receptor in the functional agonist and antagonist modes were performed; the agonist EC_{50} could not be determined due to lack of signal up to 3 μ M, and the antagonist IC_{50} was 0.75 μ M. The selectivity of 17h for human MC2R over 5-HT_{1B} is >2500-fold.

Compound 17h had a favorable ADME profile as depicted in Table 7. Like human and rat liver microsomal stability shown in Table 5, the half-life in dog liver microsomes was

long ($t_{1/2} = 173$ min). Compound 17h displayed low levels of hERG binding and a favorable CYP profile. In MDR1-MDCK cell monolayers, 17h showed modest apparent permeability (1.9×10^{-6} cm/s) and had a high efflux ratio (95), suggesting that 17h is a P-gp substrate. Relatively high lipophilicity of 17h ($\log P = 4.75$, experimental value) was reflected by relatively high plasma protein binding in human and rat (1.4–2.6% free fraction) but moderate binding in dog (~13% free fraction).

Despite the modest permeability of 17h, pharmacokinetic studies showed that 17h had good plasma exposure, moderate systemic clearance, low steady-state volume of distribution, and good to excellent oral bioavailability in rat and dog, respectively (Table 8).

The in vivo pharmacodynamic effect of compound 17h was evaluated in an ACTH-stimulated corticosterone secretion model in male rats. Compound 17h suppressed ACTH-stimulated corticosterone at 1 h (44% and 88% with 3 and 30 mg/kg, respectively) and 4 h (36% and 84% with 3 and 30 mg/kg, respectively) postoral administration compared to vehicle treatment (Figure 2). The time course and magnitude of the effect were consistent with the presence of 17h detected in the plasma (Table 9). ACTH-stimulated corticosterone returned to normal levels at 24 and 48 h after a single oral administration of 3 or 30 mg/kg 17h as expected based on the absence or low plasma concentrations of 17h at these time points.

In summary, to our knowledge, we have discovered the first novel series of potent and selective MC2R antagonists. The overall SAR process led to the discovery of compound 17h (CRN04894), which possesses a satisfactory pharmaceutical profile including pharmacokinetic properties, efficacy, and safety. Compound 17h was selected as a candidate to further characterize its potential for clinical utility. Recently, 17h was evaluated in healthy volunteers for pharmacokinetics, pharmacodynamics, and tolerability¹⁴ and is currently being evaluated in clinical trials to potentially become a first-in-class treatment for CAH and Cushing's disease. The outcome of further studies will be reported in due course.

■ ASSOCIATED CONTENT


Supporting Information

The Supporting Information is available free of charge at <https://pubs.acs.org/doi/10.1021/acsmmedchemlett.3c00514>.

Synthesis and analytical data for selected key compounds (**8e**, **9a**, **10a**, **16n**, **16o**, **17h** (CRN04894)), representative in vitro and in vivo assay protocols, and additional data for CRN04894 (PDF)


■ AUTHOR INFORMATION

Corresponding Author

Sun Hee Kim – Crinetics Pharmaceuticals, Inc., San Diego, California 92121, United States;  orcid.org/0009-0002-0104-2109; Email: skim@crinetics.com

Authors

Sangdon Han – Crinetics Pharmaceuticals, Inc., San Diego, California 92121, United States; Present Address: Crossignal Therapeutics

Jian Zhao – Crinetics Pharmaceuticals, Inc., San Diego, California 92121, United States;  orcid.org/0000-0002-7544-8331

Shimiao Wang – Crinetics Pharmaceuticals, Inc., San Diego, California 92121, United States

Ana Karin Kusnetzow – Crinetics Pharmaceuticals, Inc., San Diego, California 92121, United States; Present Address: Radionetics Oncology.

Greg Reinhart – Crinetics Pharmaceuticals, Inc., San Diego, California 92121, United States; Present Address: Radionetics Oncology.

Melissa A. Fowler – Crinetics Pharmaceuticals, Inc., San Diego, California 92121, United States

Stacy Markison – Crinetics Pharmaceuticals, Inc., San Diego, California 92121, United States

Michael Johns – Crinetics Pharmaceuticals, Inc., San Diego, California 92121, United States

Rosa Luo – Crinetics Pharmaceuticals, Inc., San Diego, California 92121, United States

R. Scott Struthers – Crinetics Pharmaceuticals, Inc., San Diego, California 92121, United States

Yunfei Zhu – Crinetics Pharmaceuticals, Inc., San Diego, California 92121, United States; Present Address: Radionetics Oncology.

Stephen F. Betz – Crinetics Pharmaceuticals, Inc., San Diego, California 92121, United States

Complete contact information is available at:

<https://pubs.acs.org/doi/10.1021/acsmmedchemlett.3c00514>

Funding

This work was supported in part by an SBIR grant from the NIH awarded to R.S.S. (R43-DK115245).

Notes

The authors declare the following competing financial interest(s): All authors are employees of Crinetics Pharmaceuticals, Inc., except S.H. and G.R. who were previous employees and A.K.K. and Y.Z. who were also previous employees and are currently consultants for Crinetics.

■ ACKNOWLEDGMENTS

We thank Julie Nguyen, Christine Staley, and Hannah Liu for in vitro assays, Taylor Kredel and Jon Athanacio for in vivo assays, and Jeff Schkeryantz for proofreading the manuscript.

■ ABBREVIATIONS

MC2R, melanocortin type 2 receptor; SAR, structure–activity relationship; CD, Cushing's disease; CAH, congenital adrenal hyperplasia; HPA, hypothalamic-pituitary-adrenal; ACTH, adrenocorticotrophic hormone; HATU, 1-[bis(dimethylamino)methylene]-1H-1,2,3-triazolo[4,5-b]pyridinium-3-oxide hexafluorophosphate; THF, tetrahydrofuran; AL, advanced lead; EW, electron withdrawing; ED, electron donating; ADME, absorption, distribution, metabolism, and excretion; hERG, human ether-à-go-go-related gene; CYP, cytochrome P450

■ REFERENCES

- (1) Gjerstad, J. K.; Lightman, S. L.; Spiga, F. Role of glucocorticoid negative feedback in the regulation of HPA axis pulsatility. *Stress* **2018**, *21* (5), 403–416.
- (2) Herman, J. P.; McKlveen, J. M.; Ghosal, S.; Kopp, B.; Wulsin, A.; Makinson, R.; Scheimann, J.; Myers, B. Regulation of the hypothalamic-pituitary-adrenocortical stress response. *Compr. Physiol.* **2016**, *6* (2), 603–621.
- (3) Sharma, S. T.; Nieman, L. K.; Feelders, R. A. Cushing's syndrome: epidemiology and developments in disease management. *Clin. Epidemiol.* **2015**, *7*, 281–293.
- (4) White, P. C.; Speiser, P. W. Congenital adrenal hyperplasia due to 21-hydroxylase deficiency. *Endocr. Rev.* **2000**, *21* (3), 245–291.
- (5) Speiser, P. W.; Arlt, W.; Auchus, R. J.; Baskin, L. S.; Conway, G. S.; Merke, D. P.; Meyer-Bahlburg, H. F. L.; Miller, W. L.; Murad, M. H.; Oberfield, S. E.; White, P. C. Congenital adrenal hyperplasia due to steroid 21-hydroxylase deficiency: an endocrine society clinical practice guideline. *J. Clin. Endocrinol. Metab.* **2018**, *103* (11), 4043–4088.
- (6) Berglund, A.; Ornstrup, M. J.; Lind-Holst, M.; Dunø, M.; Bækvad-Hansen, M.; Juul, A.; Borch, L.; Jørgensen, N.; Rasmussen, A. K.; Andersen, M.; Main, K. M.; Hansen, D.; Gravholt, C. H. Epidemiology and diagnostic trends of congenital adrenal hyperplasia in Denmark: a retrospective, population-based study. *Lancet Reg. Health Eur.* **2023**, *28*, 100598.
- (7) Malik, S.; Dolan, T. M.; Maben, Z. J.; Hinkle, P. M. Adrenocorticotrophic hormone (ACTH) responses require actions of the melanocortin-2 receptor accessory protein on the extracellular surface of the plasma membrane. *J. Biol. Chem.* **2015**, *290* (46), 27972–27985.
- (8) For an example of an MC2R antagonist without disclosure of the structure, see: Forfar, R.; Hussain, M.; Khurana, P.; Cook, J.; Lewis, S.; Popat, D.; Jackson, D.; McIver, E.; Jerman, J.; Taylor, D.; Clark, A. J.; Chan, L. F. Identification of a novel specific small-molecule melanocortin-2-receptor antagonist. *Endocr. Connect.* **2022**, *11* (12), e220338.
- (9) Yang, Y. Structure, function and regulation of the melanocortin receptors. *Eur. J. Pharmacol.* **2011**, *660* (1), 125–130.
- (10) Jiang, W.; Tucci, F. C.; Tran, J. A.; Fleck, B. A.; Wen, J.; Markison, S.; Marinkovic, D.; Chen, C. W.; Arellano, M.; Hoare, S. R.; Johns, M.; Foster, A. C.; Saunders, J.; Chen, C. Pyrrolidinones as potent functional antagonists of the human melanocortin-4 receptor. *Bioorg. Med. Chem. Lett.* **2007**, *17* (20), 5610–5613.
- (11) Jiang, W.; Tucci, F. C.; Chen, C. W.; Arellano, M.; Tran, J. A.; White, N. S.; Marinkovic, D.; Pontillo, J.; Fleck, B. A.; Wen, J.; Saunders, J.; Madan, A.; Foster, A. C.; Chen, C. Arylpropionylpiperazines as antagonists of the human melanocortin-4 receptor. *Bioorg. Med. Chem. Lett.* **2006**, *16* (17), 4674–4678.
- (12) We confirmed MC2 selective antagonistic activity from a derivative of compound **2**. Antagonistic activity of compound **8e** at 10 μ M concentration: MC2 Δ pEC₅₀ = 2.6 and MC4 Δ pEC₅₀ = 0.0.
- (13) Kusnetzow, A. K.; Fowler, M. A.; Athanacio, J.; Reinhart, G.; Rico-Bautista, E.; Han, S.; Kim, S. H.; Johns, M.; Kredel, T. A.; Nguyen, J.; Staley, C.; Tan, H.; Luo, R.; Markison, S.; Madan, A.; Zhu, Y. F.; Struthers, S.; Betz, S. F. SAT-364 Nonpeptide orally

bioavailable ACTH antagonists: Suppression of ACTH-induced corticosterone secretion and adrenal hypertrophy in rats. *J Endocr Soc.* **2019**, 3, SAT-364.

(14) Trainer, P. J.; Ferrara-Cook, C. T.; Ayala, A.; Luo, R.; Miller, S.; Wang, Y.; Hernandez-Illas, M.; Struthers, R. S.; Betz, S. F.; Krasner, A. CRN04894: an oral, nonpeptide ACTH (MC2) receptor antagonist decreased basal and stimulated cortisol secretion in healthy volunteers. In *Society for Endocrinology BES 2022*, November 14–16, Harrogate, England.